Sirodesmin PL Dithioacetal 7 from Dithiol 8. The dithiol **8** was prepared as already described by reduction of the natural disulfide **3** (486 mg, 1 mmol) with an excess of methanethiol in dry pyridine at 0 °C.

The reaction mixture was then dried under reduced pressure and the residue was dissolved in 10 mL of methylene chloride. The solution was treated with 165 mg of *p*-anisaldehyde (1.2 mmol) and 0.2 mL of boron trifluoride etherate and allowed to stand at room temperature for 3 h. Direct separation of the solution on a silica gel cake (eluted by increasing gradient of ethyl acetate in methylene chloride) afforded 520 mg (86%) of the diastereomeric mixture of *syn*- (90%) and *anti*- (10%) thioacetals **7**.

As precedingly, the major syn isomer was purified by recrystallizations in ethanol: mp 192–193 °C; $[\alpha]^{20}_D$ −31° (*c* 0.5 in methanol).

All physicochemical and spectroscopic properties of this material were identical with those obtained for the *syn*-dithioacetal precedingly prepared from the monosulfide **4**.

The stereochemistry as well as the proportion of afforded syn and anti diastereoisomers of **7** was deduced from the NMR spectrum of the purified reaction mixture: signals of NMe, H-7, and Ar CH hydrogens were analyzed δ respectively 3.30, 5.26, and 5.08 for the syn and 3.16, 5.51, and 5.28 for the anti isomer.

6,14-Diacetylmonodethiosirodesmin PL 12. A mixture of 227 mg (0.5 mmol) of the monosulfide **4**, 3 mL of pyridine, and 2 mL of acetic anhydride was allowed to stand at room temperature for 48 h. The solution was evaporated under reduced pressure, and a subsequent TLC purification step (ethyl acetate–methylene chloride 1:4) gave, beside a minor amount of **11**, 197 mg (73%) of pure diacetate **12**: mp 195–197 °C (methylene chloride–hexane); λ_{max} (methanol) 215 (ϵ 5.17 × 10^3) and 262 nm (ϵ 2.1 × 10^3); CD (methanol) $\Delta\epsilon_{211nm}$ = +31.3, $\Delta\epsilon_{248nm}$ = +4.9, $\Delta\epsilon_{276nm}$ = −14.8, and $\Delta\epsilon_{328nm}$ = +0.3; ν_{max} (CCl_4) 1765, 1730, and 1210–1230 cm^{-1}; δ ($CDCl_3$) 0.93 and 1.01 (6 H, 2 s, Me-16 and Me-17), 1.27 (3 H, d, *J* = 6.5 Hz, Me-18), 2.08 and 2.32 (2 H, 2 dd, *J* = 14.5, 1.5, and 8.8 Hz, CH_2-12), 2.03, 2.10, and 2.15 (9 H, 3 s, 3 OCOMe), 3.00 (3 H, s, NMe), 3.21 (2H, s, CH_2-5), 3.80 (1 H, q, *J* = 6.5 Hz, H-11), 4.73 and 4.87 (2H, AB q, *J* = 13.8 Hz, CH_2-14), 4.34 (1 H, dd, *J* = 1.5 and 8.8 Hz, H-13) and 5.68 (1 H, s, H-7); MS (EI) 538 (17, M), 481 (46), 478 (15), 435 (14), 418 (55), 361 (100) 302 (71), 114 (86), and 94 (95).

X-ray Analysis of 12. **12** gave suitable crystals for X-ray analysis from the mixture carbon tetrachloride–methylene chloride. The compound crystallized with one molecule of carbon tetrachloride in the monoclinic form. The crystal used for the X-ray structure determination was a white prism whose dimensions were 0.7 × 0.3 × 0.2 mm. The final results obtained are presented in the supplementary material.

Methoxy Thiol 14. To a solution of 243 mg of sirodesmin PL (**3**) in 20 mL of dry methanol was added 145 mg of triphenylphosphine (1.1 equiv) at 0 °C. A minimum of methylene chloride was added to the reaction mixture until complete dissolution was obtained. After standing at room temperature for 1 h, the solution was evaporated and the residue submitted to a silicic acid column chromatography. Elution with methylene chloride–ethyl acetate 2:3 gave 187 mg (76%) of methoxy thiol **14**: MS (EI) 486 (1, M), 455 (27), 454 (40), 453 (15), 423 (27), 421 (28), 397 (40) and 158 (100%); δ ($CDCl_3$) 1.03 and 1.12 (6 H, 2 s, Me-16 and Me-17), 1.28 (3 H, d, *J* = 6.5 Hz, Me-18), 2.02 and 2.84 (2 H, 2 dd, *J* = 14, 9.2, and 9 Hz, CH_2-12), 2.09 (3 H, s, OCOMe), 2.69 and 3.37 (2 H, AB q, *J* = 15 Hz, CH_2-5), 3.06 (3 H, s, NMe), 3.36 (3 H, s, OMe), 4.01 (1 H, q, *J* = 6.5 Hz, H-11) 3.79 and 4.21 (2 H, AB q, *J* = 12 Hz, CH_2-14), 4.51 (1 H, dd, *J* = 9 and 9.2 Hz, H-13) and 5.90 (1 H, s, H-7).

Registry No. 3, 64599-26-4; **4**, 86258-54-0; *syn*-**7**, 86197-02-6; *anti*-**7**, 86286-47-7; **8**, 86197-03-7; **11**, 86197-05-9; **12**, 86197-04-8; **14**, 86217-12-1; **15**, 86197-06-0; **16**, 86197-07-1; anisaldehyde, 123-11-5; anisaldehyde (trithiane derivative), 5692-49-9.

Supplementary Material Available: Additional experimental details, figures of structures and dihedral angles, and tables of structural and spectroscopic data (17 pages). Ordering information is given on any current masthead page.

Conformational Analysis of Functionalized Sultines by Nuclear Magnetic Resonance and X-ray Crystallography. Application of a Generalized Karplus Equation

C. A. G. Haasnoot,[1a] R. M. J. Liskamp,*[1b] P. A. W. van Dael,[1a] J. H. Noordik,[1c] and H. C. J. Ottenheijm*[1b]

Contribution from the Departments of Organic Chemistry, Biophysical Chemistry, and Crystallography, University of Nijmegen, Toernooiveld, 6525 ED Nijmegen, The Netherlands.
Received November 22, 1982

Abstract: The *solid-state* conformation of the β-amino-γ-sultine **2** was determined by X-ray crystallography, which allowed also the assignment of the *R* configuration to the sulfinate sulfur atom. In addition the conformation of compounds **1** and **2** *in solution* is reported. This conformational analysis is based on the application of a new, empirical generalization of the classical Karplus equation. Application of eq 1 and 4 allowed the expression of vicinal coupling constants—obtained by 500-MHz NMR spectroscopy—in proton–proton torsion angles φ_{HH}. The puckering and conformation of the sultine ring of **1** and **2** are quantitatively described by using the concept of pseudorotation (eq 1, **2a–d**). It appeared that in $CDCl_3$ at 233 or 300 K compound **1** is present as a twist-chair conformer, which can be denoted as $^4T_5$ (Scheme I). In Me_2SO-d_6 compound **1** is engaged in an equilibrium between this $^4T_5$ conformer and another twist-chair conformer, denoted at ^3_2T. Compound **2** in $CDCl_3$ at 233 K is engaged in two conformational equilibria, a slow and a fast one on the NMR time scale. The slow equilibrium between a major component and a minor component is due to hindered rotation in the urethane side chain. In the fast equilibrium the five-membered ring is engaged in an equilibrium between a twisted chair conformer (^4_3T) and an envelope-shaped conformer ($_1E$, see Scheme II). The slow equilibrium is not observed in Me_2SO-d_6 at 300 K or in $C_2D_2Cl_4$ at 383 K. The effects that might play a role in determining the conformation of **1** and **2** in solution are the gauche effect (Figure 7), the anomeric effect (Figure 8), and hydrogen bonding. Hydrogen bonding governs the solid-state conformation of **2**, an envelope-shaped ($_3E$) conformer (Figure 3). Thus, a comparison of the solution conformer and the solid-state conformer of **2** (Scheme II and Figure 3, respectively) shows a remarkable difference.

Recently, we reported[2] an efficient route leading to the functionalized five-membered cyclic sulfinate esters—γ-sultines—**1–3** and found that nucleophilic ring-opening reactions of these sultines proceed with inversion at sulfur. This finding was based on the

0002-7863/83/1505-5406$01.50/0

establishment of the absolute configuration of one of the sultines used. In the same report we established[2] that the chiral sulfur atom causes chiral induction in ring-opening reactions with a prochiral nucleophile.[3] For a fundamental understanding of this chiral induction, insight into the conformation of the sultines in solution is a prerequisite. Therefore, we now present the crystallographic analysis of the solid-state conformation, as well as the conformational analysis of **2** and **3** in solution. The latter analysis is a new application of a generalized form of the Karplus equation, which has been formulated[4] and utilized successfully in previous investigations.[5]

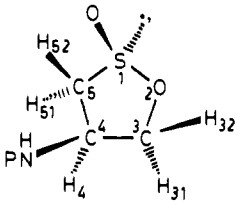

R_C,S_S

1, P = BOC

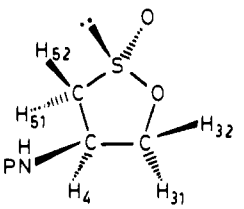

R_C,R_S

2, P = BOC
3, P = CbO
4, P = $C_6H_5(CH_2)_2CO$

Methods

Pseudorotation Analysis of the Sultine Ring. In general the conformation of a five-membered ring is conveniently described by using the concept of pseudorotation.[6,7] The endocyclic torsion angles Φ_j of a five-membered ring are interrelated via the pseudorotation eq 1 in which $j = 0$–4. The puckering and conformation

$$\Phi_j = \Phi_m \cos (P + 4\pi j/5) \quad (1)$$

of the sultine ring may thus be described quantitatively by two parameters: P is the phase angle of pseudorotation and Φ_m is the puckering amplitude. The endocyclic torsion angle of the bond opposite to the sulfur atom is defined as the reference angle Φ_0; the remaining torsion angles Φ_1, Φ_2, Φ_3, and Φ_4 are assigned clockwise to C4–C5, C5–S1, S1–O2, and O2–C3, respectively (see structure **5**). By application of a new empirical generalization

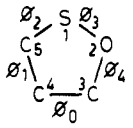

5

of the classical Karplus equation (vide infra, eq 4), experimental vicinal ^{1}H NMR coupling constants can be correlated with proton–proton torsion angles φ_{HH}. These torsion angles are intimately related to the endocyclic torsion angles Φ_j, which, in turn, determine the pseudorotation parameters P and Φ_m (eq 1). Therefore, in order to determine the conformation of the sultine ring in terms of the pseudorotation concept, correlations between the pseudorotation parameters (P and Φ_m) and the proton–proton torsion angles are called for.

Table I. Bond Distances (with Esd's, Å) of 2

atoms	d	$\langle d \rangle$	atoms	d
S1–O6	1.466 (7)	1.460	S1′–O6′	1.453 (7)
S1–O2	1.586 (7)	1.592	S1′–O2′	1.598 (6)
S1–C5	1.780 (7)	1.807	S1′–C5′	1.833 (9)
O2–C3	1.426 (11)	1.415	O2′–C3′	1.403 (8)
C3–C4	1.524 (11)	1.515	C3′–C4′	1.505 (11)
C4–C5	1.525 (11)	1.534	C4′–C5′	1.543 (10)
C4–N7	1.402 (9)	1.418	C4′–N7′	1.434 (9)
N7–C8	1.356 (7)	1.355	N7′–C8′	1.354 (7)
C8–O11	1.189 (7)	1.195	C8′–O11′	1.201 (7)
C8–O9	1.332 (7)	1.327	C8′–O9′	1.321 (8)
O9–C10	1.484 (7)	1.483	O9′–C10′	1.482 (7)
C10–C12	1.503 (9)	1.495	C10′–C12′	1.487 (10)
C10–C13	1.491 (10)	1.512	C10′–C13′	1.533 (11)
C10–C14	1.513 (10)	1.502	C10′–C14′	1.490 (11)

[a] The esd's result from the least-squares refinement and are probably underestimated because of the decomposition of the crystal during the measurements.

A complication arises, however, because the pseudorotation equation (1) can only be regarded as near exact for *equilateral* five-membered rings like cyclopentane. In heterocyclic systems with varying endocyclic bond distances, as is pertinently the case for the sultine ring under study (bond distances from 1.40 to 1.83 Å, Table I) eq 1 is expected to *reproduce* the endocyclic torsion angles—and hence the exocyclic proton–proton torsion angles—only with limited accuracy. Indeed, this expectation is borne out by experiment as the torsion angles recalculated from the pseudorotation parameters for the sultine ring in the solid state (vide infra) show deviations up to 2.5° when compared with the experimentally observed torsion angles. Recently, eq 1 was improved by de Leeuw et al.[8] by introducing two correction factors.

This corrected pseudorotation equation yields the following correlations between the proton–proton torsion angles φ_{HH} and the pseudorotation parameters governing the conformation of the sultine ring (eq 2a–d). Obviously, by combining eq 1 and 2a–d,

$$\varphi_{31-4} = -3.9 + 1.0033\Phi_m \cos (P - 2.48) \quad (2a)$$

$$\varphi_{32-4} = -123.3 + 1.0033\Phi_m \cos (P - 2.48) \quad (2b)$$

$$\varphi_{4-51} = 4.0 + 1.0206\Phi_m \cos (P + 140.72) \quad (2c)$$

$$\varphi_{4-52} = 123.2 + 1.0206\Phi_m \cos (P + 140.72) \quad (2d)$$

it will suffice—at least in theory—to determine two vicinal coupling constants in order to give a full description of the five-membered ring in terms of P and Φ_m. When more coupling constants and hence more torsion angles are known, the system is overdetermined and "best" values for P and Φ_m may be obtained either by averaging or, preferably, by least-squares fitting of the data.

Another complication may arise when the five-membered ring under study is engaged in a fast equilibrium between two distinct conformers; then the experimental coupling constants ^3J represent time-average values that are linearly related to the coupling constants of the individual conformers $J(I)$ and $J(II)$ and their populations as expressed by eq 3, where x is the mole fraction of conformer I.

$$^3J_{exptl} = xJ(I) + (1 - x)J(II) \quad (3)$$

In this case the complete conformational analysis entails the determination of five independent parameters $P(I)$, $\Phi_m(I)$, $P(II)$, $\Phi_m(II)$, and x from the observed coupling constants. This objective

(1) (a) Department of Biophysical Chemistry. (b) Department of Organic Chemistry. (c) Department of Crystallography.
(2) Liskamp, R. M. J.; Zeegers, H. J. M.; Ottenheijm, H. C. J. *J. Org. Chem.* **1981**, *46*, 5408.
(3) Induction by a chiral sulfur has also been observed with noncyclic sulfinate esters: Annunziata, R.; Cinquini, M.; Colonna, S.; Cozzi, F. *J. Chem. Soc., Perkin Trans. 1* **1981**, 614. So far, it has not been studied with the conformationally more rigid sultines.
(4) Haasnoot, C. A. G.; de Leeuw, F. A. A. M.; Altona, C. *Tetrahedron* **1980**, *36*, 2789.
(5) (a) Haasnoot, C. A. G.; de Leeuw, F. A. A. M.; de Leeuw, H. P. M.; Altona, C. *Recl. Trav. Chim. Pays-Bas* **1979**, *98*, 576. (b) Haasnoot, C. A. G.; de Leeuw, F. A. A. M.; Altona, C. *Bull. Soc. Chim. Belg.* **1980**, *89*, 125. (c) Haasnoot, C. A. G.; de Leeuw, F. A. A. M.; de Leeuw, H. P. M.; Altona, C. *Org. Magn. Reson.* **1981**, *15*, 43. (d) Haasnoot, C. A. G. de Leeuw, F. A. A. M.; de Leeuw, H. P. M.; Altona, C. *Biopolymers* **1981**, *20*, 1211. (e) Birnbaum, G. I.; Gygler, M.; Ekield, I.; Shugar, D.; *J. Am. Chem. Soc.* **1982**, *104*, 3957.
(6) Kilpatrick, J. E.; Pitzer, K. S.; Spitzer, R.; *J. Am. Chem. Soc.* **1947**, *69*, 2483, Pitzer, K. S.; Donath, W. E. *Ibid.* **1959**, *81*, 3213.
(7) Altona, C.; Buys, H. R.; Havinga, E. *Recl. Trav. Chim. Pays-Bas* **1966**, *85*, 973. Altona, C.; Geise, H. J.; Romers, C. *Tetrahedron* **1968**, *24*, 13. Altona, C.; Sundaralingam, H. *J. Am. Chem. Soc.* **1972**, *94*, 8205.
(8) de Leeuw, F. A. A. M.; van Kampen, P. N.; Diez, E.; Esteban, A. L.; Altona, C. submitted for publication.

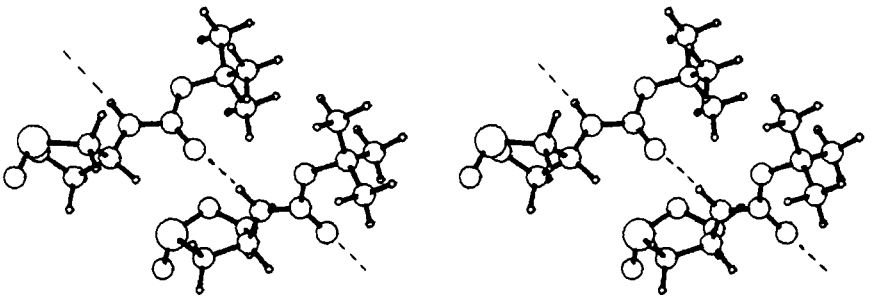

Figure 1. Spectroscopic view of **2** in the unit cell.

was realized by an iterative least-squares computer program (written in PASCAL) devised to obtain the best fit of the equilibrium parameters to the experimental coupling constants. At this point it should be mentioned that for the sultine ring under study the system is in fact underdetermined as only four observables—i.e., coupling constants—are available from experiment for the calculation of $\Phi_m(I)$, $P(I)$, $\Phi_m(II)$, $P(II)$, and x. Therefore, within each minimization one or more parameters must be constrained to reasonable values. In the following sections it will be demonstrated that the procedure outlined above yields a consistent conformational analysis of the sultine ring in solution.

Determination of the Proton–Proton Torsion Angles. To obtain the proton–proton torsion angles necessary for the pseudorotation analysis of the sultine ring (eq 1, 2a–d), a new empirical generalization[4] of the classical Karplus equation was used.

In this generalized equation the standard Karplus equation is extended with correction terms in order to described the influence of electronegative substitutents on vicinal coupling constants in an explicit way. Each H–C–C–H fragment in the ring of compounds **1** and **2** carries three non-hydrogen substituents in which case the generalized equation takes the form

$$^3J_{HH} = 13.22\cos^2\varphi - 0.99\cos\varphi + \sum\Delta\chi_i\{0.87 - 2.46\cos^2(\xi_i\varphi + 19.9|\Delta\chi_i|)\} \quad (4)$$

The first two terms describe the dependency of the vicinal coupling constant ($^3J_{HH}$) in the H–C–C–H fragment under study on the Klyne–Prelog signed proton–proton torsion angle.[9] The remaining terms account for the dependency of $^3J_{HH}$ on the electronegative substituent S_i; these terms depend on the torsion angle φ, on the differences in electronegativity between the substituents S_i and hydrogen on the Huggins scale[10] ($\Delta\chi_i$), and finally on the orientation of the substituent S_i with respect to the coupling protons[4] (ξ_i).

Results

X-ray Crystallographic Analysis of 2. In order to determine the configuration of the sulfoxide–sulfur atom and the solid-state conformation of the ring, a single-crystal X-ray structure determination of **2** was performed (see also Experimental Section). The compound crystallized from dichloromethane/carbon tetrachloride as monoclinic needles having two crystallographically independent molecules in the unit cell; see Figure 1.

The two molecules possess the same configuration (vide infra); most of the corresponding bond distances (Table I) and angles agree within the accuracy of the structure determination. The larger differences are partly ascribed to the diminishing quality of the crystal; we do not affix structural significance to these differences. The structure of the molecules is shown in Figure 2. By reference to the chiral carbon atom having the R configuration (see Experimental Section), the chiral sulfur atom can readily be seen to possess the R configuration[11] also. The C5–S1 bond is, as expected, the longest bond in the ring of both molecules

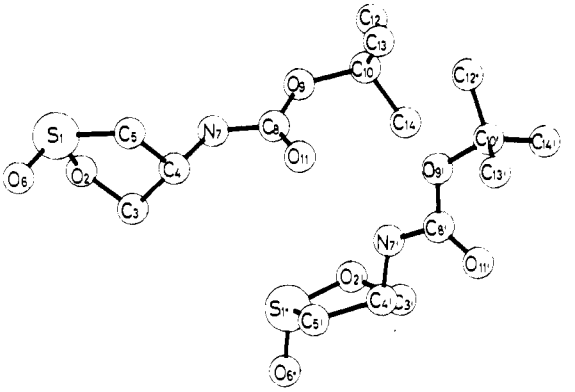

Figure 2. X-ray analysis of **2** showing the R_C–R_S configuration.

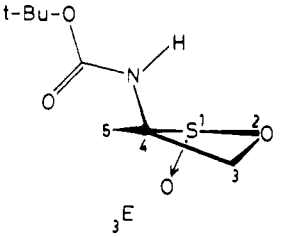

Figure 3. Representation of **2** in the solid state showing the envelope shape $_3E$.

Table II. Chemical Shift Data (ppm) of **1** in Different Solvents and at Different Temperatures

proton	$CDCl_3$ 233 K	$CDCl_3$ 300 K	Me_2SO-d_6 300 K
H_{31}	4.659	4.623	4.572
H_{32}	4.810	4.749	4.511
H_4	4.955	4.899	4.433
H_{51}	3.021	2.972	3.481
H_{52}	3.294	3.201	2.994
H_N	6.154	6.012	7.040
$H_{t\text{-}Bu}$	1.438	1.437	1.390

in the unit cell; its values (1.780 and 1.833 Å) are similar to those reported for nonfunctionalized sultines.[12,13]

In Figure 1 the presence of intermolecular hydrogen bonds between NH and C=O is indicated. The observed O–N distances are 2.88 and 2.93 Å, and the corresponding N–H–O angles are 156 and 150°, respectively. Consequently, the hydrogen bonds can be classified as moderately strong.[14] Due to these hydrogen bonds the molecules form straight chains throughout the crystal.

(9) Klyne, W.; Prelog, V. *Experientia* **1960**, *16*, 521.
(10) Huggins, M. L. *J. Am. Chem. Soc.* **1953**, *75*, 4123.
(11) The *R*/*S* nomenclature as adopted for sulfinate esters (Mislow, K.; Green, J. M.; Laur, P.; Mellilo, J. T.; Simmons, T.; Ternay, A. L., Jr. *J. Am. Chem. Soc.* **1965**, *87*, 1958) has been followed here, in that the S–O "double" bond has a lower priority than the S–OR bond.
(12) Surcouf, E. *Acta Crystallogr., Sect. B* **1979**, *B35*, 1922; *Ibid.* **1979**, *B35*, 1925.
(13) Spek, A. L. *Cryst. Struct. Commun.* **1979**, *8*, 127.
(14) Hamilton, W. C.; Ibers, J. A. "Hydrogen Bonding in Solids"; W. A. Benjamin: New York, 1968.

Table III. Coupling Constant Data (Hz) of **1** in Different Solvents and at Different Temperatures

coupling	$CDCl_3$, 233 K			$CDCl_3$, 300 K			Me_2SO-d_6, 300 K		
	J_{exptl}	J_{calcd}	ΔJ	J_{exptl}	J_{calcd}	ΔJ	J_{exptl}	J_{calcd}[a]	ΔJ
H_{31-4}	5.82	5.80	0.02	5.93	5.96	−0.03	6.68	6.72	−0.04
H_{32-4}	1.52	1.48	0.04	1.74	1.54	0.20	5.22	5.26	−0.04
H_{51-4}	7.00	7.05	−0.05	7.21	7.18	0.03	8.21	8.12	0.09
H_{52-4}	0.90	1.22	−0.32	0.99	1.22	−0.23	3.53	3.50	0.03
H_4-NH	9.9			8.2			6.0		
H_{31-32}	−9.67			−9.67			−8.92		
H_{51-52}	−13.14			−13.15			−13.41		

[a] Calculated for a conformational equilibrium (see text).

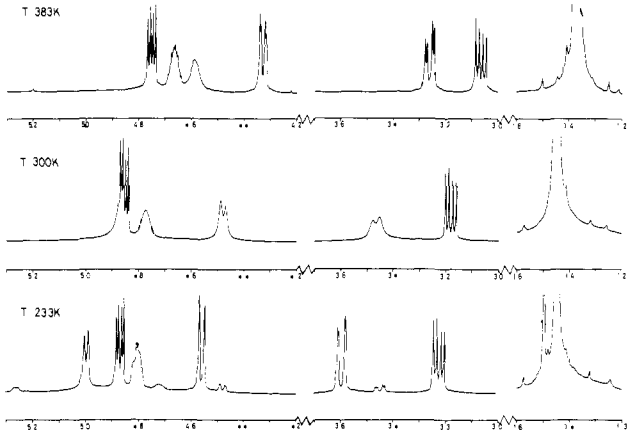

Figure 4. 500-MHz ^1H NMR spectrum of **2** in $CDCl_3$ at 233 K and at 300 K and in $C_2D_2Cl_4$ at 383 K.

The conformation of the ring of **2** in the unit cell can be described in terms of pseudorotation as has been outlined above (eq 1). As a result the two sultine rings in the unit cell have phase angles of pseudorotation (P) of 334.7 and 332.7° with puckering amplitudes (Φ_m) of 44.6 and 44.7°, respectively. Both conformations are almost envelope shaped, with C3 out of the plane and pointing into the direction opposite to the C4–N bond, a conformation which is denoted[15] by ${}_3E$ (Figure 3). An alternative way to describe the envelope-shaped conformation is the dihedral angle between the planes through the atoms [C4, C5, S1, O2] and [C4, C3, O2]; this value is 41° for both molecules in the unit cell.

^1H NMR Spectra of 1 and 2. The proton chemical shift values of **1** measured at 500 MHz are collected in Table II. The corresponding coupling constants are listed in Table III. The 500-MHz spectra of **2** deserve some comment; the spectrum in $CDCl_3$ at 300 K, depicted in Figure 4, shows the simultaneous presence of both sharp and broad resonances. The broad resonances at δ 3.47 and 4.48 were taken indicative for chemical shift exchange phenomena. This conception was confirmed by measurements at lower temperature (233 K); the broad lines sharpen up to give two sets of signals with an integration ratio of about 9:1 (Figure 4). The Gaussian enhanced spectrum of **2** at 233 K is represented in Figure 5. Perusal of this spectrum reveals that the sharp resonances are also split into two sets of signals, displaying a similar integration ratio; however, the chemical shift differences are very small (0.01 ppm). From these observations we concluded that **2** is engaged in a slow equilibrium between two conformers; the conformer with the larger integration values for all resonances is called the *major* component and the other conformer the *minor* component. We have strong indications that the bipartition of **2** in these components originates from different coformations in the side chain and not from different ring conformations (vide infra). The chemical shift data and coupling data for the major and minor component of **2** are collected in

(15) The symbols mean the following: ${}_xE$, envelope with atom x puckered downward; ${}^y_xT$, twist-chair, with atom y puckered up and atom x puckered downward, the degree of puckering is about the same. If atom x is less puckered than atom y, ${}^yT_x$ is used. The direction of the C4–N bond is chosen upward.

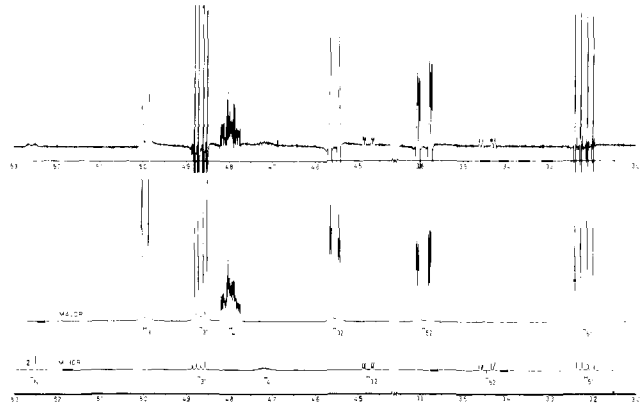

Figure 5. Gaussian enhanced experimental spectrum of **2** at 233 K and the corresponding simulated spectra of the major and minor component.

Table IV. Chemical Shift Data (ppm) of **2** in Different Solvents and at Different Temperatures

proton	$CDCl_3$, 233 K		$CDCl_3$	$C_2D_2Cl_4$	Me_2SO-d_6
	minor	major	300 K	383 K	300 K
H_{31}	4.869	4.865	4.847	4.746	4.626
H_{32}	4.475	4.554	4.474	4.323	4.332
H_4	4.717	4.798	4.78	4.660	4.566
H_{51}	3.216	3.920	3.176	3.062	3.067
H_{52}	3.443	3.590	3.461	3.256	3.432
H_N	5.259	4.994		4.581	7.327
$H_{t\text{-}Bu}$	1.495	1.445	1.445	1.383	1.388

Tables IV and V. These data and those presented in Tables II and III were obtained from computer-simulated spectra. As an example the simulated spectrum of the major and the minor component of **2** in $CDCl_3$ at 233 K is shown in Figure 5.

The assignment of the signals in the spectrum of **2** at 233 K (Figures 4 and 5) to individual protons is based on the following rationale. The urethane proton is easily recognized by its broad doublet appearance at 5 ppm and its exchange after the addition of D_2O/TFA to the sample. The singlet at high field is due to the *tert*-butyl protons. The signals in the 3.20–3.60 ppm region originate form the protons H_{51} and H_{52}; each proton gives rise to a doublet of doublets. The doublets of doublets in the 4.55–4.87 ppm region are due to the protons H_{31} and H_{32}. The multiplets due to the H_4 proton in the major and minor component are also located in this region. This global assignment is in accordance with the chemical shift data reported for the closely related compound 1,2-oxathiolane 2,2-dioxide (propane–sultone)[16] and, moreover, consistent with all observed geminal and vicinal coupling constants reported in Table V.

Assignment of the individual geminal protons at C3 and C5 is based on coupling constant considerations. Using the appropriate eq 1 and 2a–d together with the eq 4 the dependency of each of the four vicinal coupling constants on the phase angle of pseudorotation P is easily computed for two values of the puckering

(16) Ohline, R. W.; Allred, A. L.; Bordwell, F. G. *J. Am. Chem. Soc.* **1964**, *86*, 4641.

Table V. Coupling Constant Data (Hz) of 2 in Different Solvents and at Several Temperatures

	$CDCl_3$, 233 K						$C_2D_2Cl_4$, 383 K			Me_2SO-d_6, 300 K		
	minor component			major component								
coupling	J_{exptl}	J_{calcd}	ΔJ	J_{exptl}	J_{calcd}	ΔJ	J_{exptl}	J_{calcd}	ΔJ	J_{exptl}	J_{calcd}	ΔJ
H_{31-4}	4.83	5.13	−0.32	4.34	4.35	−0.01	5.16	5.47	−0.31	5.17	5.62	−0.45
H_{32-4}	2.27	2.27	−0.00	1.25	1.71	−0.46	2.61	2.62	−0.01	2.82	2.86	−0.04
H_{51-4}	6.61	6.47	0.14	6.69	6.59	0.10	6.71	6.58	0.13	6.79	6.60	0.19
H_{52-4}	3.59	3.39	0.20	2.25	2.01	0.24	4.03	3.91	0.12	4.30	4.12	0.18
H_4-NH	7.94			7.95			6.00			4.99		
H_{31-32}	−10.00			−10.16			−9.82			−9.25		
H_{51-52}	−13.82			−14.23			−13.67			−13.66		
H_{32-52}				0.99								

Table VI. Pseudorotation Parameters of 1 in Different Solvents and at Different Temperatures

			P(I), deg	Φ_m(I), deg	x		P(II), deg	Φ_m(II), deg
$CDCl_3$	233 K	1a, $^4T_5$	25	34	1			
$CDCl_3$	300 K	1b, $^4T_5$	26	33	1			
Me_2SO-d_6	300 K	1c, $^4T_5$	25	34	0.56	1d, ^3_2T	146	40

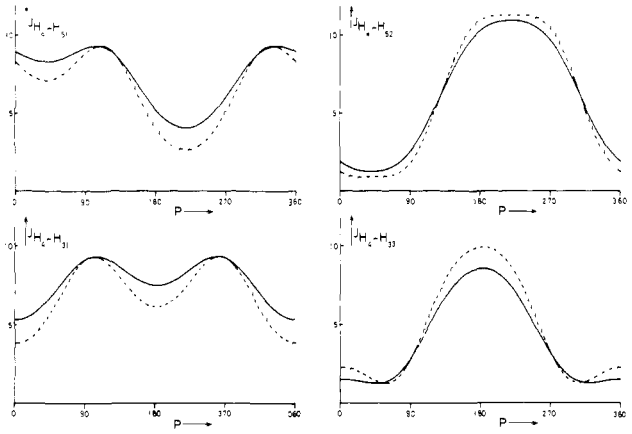

Figure 6. Calculated coupling constant profiles $^3J_{HH}$ (Hz) for 1 and 2 as a function of the pseudorotation phase angle P: solid curves, Φ_m = 35°; dashed curves, Φ_m = 45°.

amplitude, viz., 35 and 45°.[17] The resulting coupling constant profiles are shown in Figure 6. Figure 6 allows the assignment of the C3 and the C5 protons: only H_{32} and H_{52} can adopt—for certain ranges of P—coupling constant values less than or equal to 3 Hz. Consequently, those signals that correspond to a vicinal coupling constant of about 2 Hz (see Table V) can be assigned to the protons H_{32} and H_{52}.

The same line of reasoning can be used to assign the signals in the spectrum of 1 in $CDCl_3$ (Tables II and III). In Me_2SO-d_6, however, protons H_{31} and H_{32} display vicinal coupling constants of roughly the same magnitude (~6 Hz). In this case we had recourse to a solvent mixture technique: by recording the NMR spectra in mixtures of $CDCl_3$ and Me_2SO-d_6 of varying composition, it was shown that H_{31} and H_{32} as well as H_{51} and H_{52} interchange position in the spectrum when the Me_2SO-d_6 content in the solvent mixture is increased. No other assignment leads to acceptable structures in the conformational analysis (vide infra).

Solution Conformation of 1. The results of the pseudorotational analysis of 1 in $CDCl_3$ at 233 K show that the five-membered ring is best described in terms of a single conformation (**1a**) characterized by P = 25° and Φ_m = 34° (Scheme I; see also Table VI). Raising the temperature to 300 K hardly effects the experimental coupling constants: again a comparable conformation (**1b**) described by P = 26° and Φ_m 33° is found. Substantial changes in the vicinal coupling constants are induced, however, when 1 is dissolved in Me_2SO-d_6 (300 K). In this case, the observed couplings cannot be rationalized in terms of one conformation for the five-membered ring, as pilot-calculation yielded unacceptably high differences between observed and calculated coupling constants (up to 1 Hz) for the ultimately "best" single conformer. Therefore, the possibility of a conformational equilibrium (see "Methods") was considered. In order to reduce the number of parameters to be extracted from the coupling constant data, the involved puckering amplitudes Φ_m(I) and Φ_m(II) were fixed to the arbitrary[18] value of 35°.

Scheme I. Solution Conformers of 1 Present in $CDCl_3$ at 233 K (1a) and at 300 K (1b) and in Me_2SO-d_6 at 300 K (1c,d)

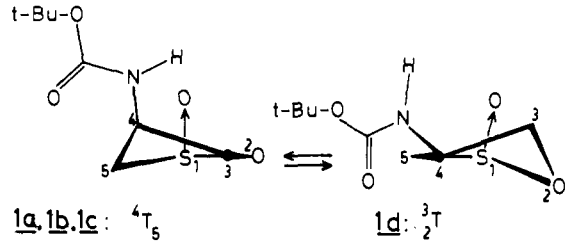

Indeed, the constrained calculation strongly indicated the existence of a conformational equilibrium characterized by P(I) = 17°, P(II) = 148°, and x = 0.54 (x = mole fraction of conformer I). Moreover, good agreement between calculated and observed coupling constants was noted (all ΔJ's < 0.1 Hz). The correspondence between one of these conformers (P(I) = 17°, Φ(I) = 35°, ^4E) and the solution conformation **1a** in $CDCl_3$ (P = 25°, Φ_m = 34°, $^4T_5$) is striking; the geometrical differences between both five-membered rings are differences of degree, not of kind. Therefore, it is not very surprising that introduction of the latter conformation **1a** as one of the components of the conformational equilibrium yields—after pseudorotational analysis—an equilibrium of **1c** ($^4T_5$) and **1d** (^3_2T) characterized by P(I) = 25°, Φ_m(I) 34°, P(II) = 146°, Φ_m(II) = 40°, and x = 0.56 (Table VI). This reproduces the observed coupling constants well (Table III).

Solution Conformation of 2. The ^{1}H NMR spectrum of 2 in $CDCl_3$ at 233 K shows the presence of a *major* and a *minor* component (vide supra). The major and the minor component are proposed to be characterized by the presence of a trans urethane bond (^4_3T-Z and $_1E$-Z, Scheme II) and a cis urethane bond (^4_3T-E and $_1E$-E, Scheme II), respectively.

Indirect evidence can be offered for this presumption: a. Calculations show (vide infra) that nearly the same conformation of the sultine ring is present in the major and minor component. This indicates that the sultine ring itself can be excluded as the cause for the chemical exchange phenomena. b. The bipartition in a major and a minor component does not originate from dif-

(17) Most of the five-membered rings reported have a puckering amplitude, 35° < Φ_m < 45°: Fuchs, B. *Top. Stereochem.* **1978**, *10*, 29.

(18) The reason for fixing the puckering amplitudes Φ_m rather than the phase angles of pseudorotation P is clearly illustrated by Figure 6: the calculated coupling constants are markedly more sensitive to changes in P.

Table VII. Pseudorotation Parameters of 2 in Different Solvents at Different Temperatures

			P(I), deg	Φ_m(I), deg	x		P(II), deg	Φ_m(II), deg	rms
$CDCl_3$	233 K	2a, ^4_3T-Z	5	45	0.91	2b, $_1E$-Z	262	45	0.23
		2c, ^4_3T-E	7	45	0.76	2d, $_1E$-E	270	54	0.30
Me_2SO-d_6	300 K	2e, ^4_3T	5	45	0.68	2f, $_1E$	265	50	0.30
$C_2D_2Cl_4$	383 K	2g, ^4_3T	5	45	0.71	2h, $_1E$	268	54	0.20

Scheme II. Solution Conformers of 2 Present in $CDCl_3$ at 233 K (2a-d), Me_2SO-d_6 at 300 K (2e,f), and in $C_2D_2Cl_4$ at 383 K (2g,h)

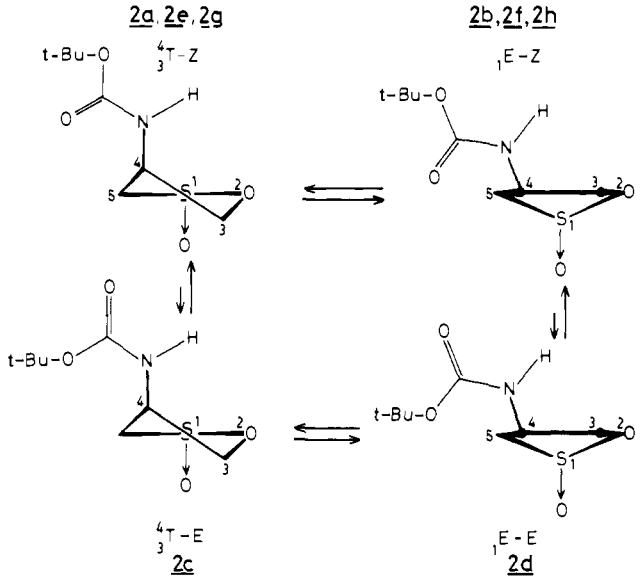

ferent conformations about the C4–N bond, as in both components vicinal proton–proton couplings H_4–C–N–H on one hand and geminal ^{13}C4–NH coupling constants on the other hand are very alike. c. The occurrence of a major and a minor component is intimately related to the presence of a urethane bond. The NMR spectra of the *N*-benzyloxycarbonylsultine **3** at 233 and 300 K display similar features. However, no chemical exchange phenomena evinced from the corresponding spectra of **4** which is a "carbon analogue" of **3**. d. Several examples of compounds containing a urethane bond are known, which exist as a pair of rotamers due to the C–N–C(O) bond (see "Discussion").

Attention is now drawn to the sultine ring of the *minor* component. Model calculations in which the *solid-state* pseudorotation parameters of **2** (P = 334°, Φ_m = 44.7°, vide supra) were introduced as a constraint did not yield satisfactory results; the residual root-mean-square (rms) deviations between the observed couplings and those calculated for the ultimately "best" conformational equilibrium remained unacceptably high (>1 Hz). Therefore, the experimental coupling constant data of the minor component were subjected to a pseudorotational analysis along the lines described for **1** in Me_2SO-d_6 (vide supra). The phase angles of pseudorotation and mole fractions in the conformational equilibrium were optimized for arbitrary puckering amplitudes, after which the puckering amplitudes were optimized. This was followed by a reoptimization of the phase angles and mole fraction. This procedure resulted in the following description of the conformational equilibrium between conformers **2c** and **2d**: P(I) = 7°, Φ_m(I) = 45°, P(II) = 270°, Φ_m(II) = 54°, and x = 0.76 (Table VII). Calculated values for the coupling constants of the ring protons in this equilibrium are listed in Table V and show good agreement with experimental values (residual root-mean-square (rms) deviation between calculated and observed couplings equals 0.23 Hz).

Similar pseudorotational analyses were carried out for the coupling constant data of the *major* component. Again, when guided by the *solid-state* conformation of **2**, no satisfactory solution was reached. However, upon introduction of the most populated conformer **2c** of the *minor* component (vide supra), the analysis smoothly optimized to a biased equilibrium of **2a** and **2b** (Scheme II) characterized by P(I) = 5°, Φ_m(I) = 45°, P(II) = 262°, Φ_m(II) = 45°, and x = 0.91 (Table VII). Subsequently, the effect of raising the temperature on the equilibrium between the major and minor component was studied, since the ^{1}H NMR spectrum in $CDCl_3$ at 300 K shows coalescence phenomena. In order to record the ^{1}H NMR spectra at elevated temperatures, the compound was dissolved in dideuteriotetrachloroethane ($C_2D_2Cl_4$). At 383 K, the minor and major component are rapidly interconverting, yielding a "time-averaged" spectrum; see Figure 4. A description of the five-membered ring in terms of an equilibrium between two conformers **2g** and **2h** (Scheme II) represented by the parameters P(I) = 5°, Φ_m(I) = 45°, P(II) = 268°, Φ_m(II) = 54°, and x = 0.71 matches the experimental coupling constants very well (rms = 0.20 Hz, see Table VII).

Remarkably, no coalescence phenomena or separation into two components could be observed when the NMR spectrum of **2** was recorded in Me_2SO-d_6 at 300 K (Tables IV and V). Either the cis–trans isomerization of the urethane bond is fast on the NMR time scale under these conditions (cf. the situation in $C_2D_2Cl_4$ at 383 K) or the equilibrium is completely one-sided in favor of one of the aforementioned rotamers. An unambiguous choice between these two possibilities cannot be made from the data at hand. Apart from this, the pseudorotational analysis of the sultine ring in this solvent appeared to be rather straightforward, yielding an equilibrium between conformers **2e** and **if** (see Scheme II) with P(I) = 5°, Φ_m(I) = 45°, P(II) = 265°, Φ_m(II) = 50°, and x = 0.68 (see Table VII).

Discussion

Although the results reported in this study allow only a qualitative insight into the specific intramolecular interactions that govern the conformational behaviour of the five-membered sultine ring, the data at hand reveal several interesting points. The molecular model constructed for the $^4T_5$ conformer of **1** (i.e., the solution conformation in $CDCl_3$, **1a**, Scheme I) suggests the facile formation of an intramolecular hydrogen bond between the NH proton and the oxygen atom of the syn S→O moiety. Sundry experimental findings support this concept: a. The N–H frequency in the IR spectrum of **1** in $CHCl_3$ is 30 cm^{-1} lower than that of the corresponding absorption in the IR spectrum of **2** having the C–N and S→O bonds in an anti arrangement (Figure 2). A similar difference in IR absorption frequency (ca. 40 cm^{-1}) has been observed in the case of 5-hydroxy-1,3-dioxane[19] and has been assigned to the presence of an intramolecular hydrogen bond. b. The NH proton in the 500-MHz NMR spectrum of **1** in $CDCl_3$ resonates at significant lower field (more than 1 ppm, cf. Tables II and IV) compared to the corresponding proton in **2**. c. The proposed intramolecular hydrogen bond in **1** in $CDCl_3$ requires an antiperiplanar position of the C4–H and N–H protons. The observed vicinal coupling constant between these protons (^3J(H_4–NH) = 9.9 Hz) is—within experimental error—equal to the maximum value (10.0 Hz) predicted by ther Karplus equation for H–C–N–H fragments given by Bystrov.[20] This indicates a complete antiperiplanar position of the protons under discussion at 233 K. When the temperature is raised to 300 K, the magnitude of the ^3J(H_4–NH) diminishes to 8.2 Hz, concomitantly the urethane amide proton shifts to higher field. These observations betoken a certain amount of disruption of the intramolecular hydrogen bonding.[21] According to the pseudorotational analysis

(19) Baggett, N.; Bukhari, M. A.; Foster, A. B.; Lehnmann, J.; Webber, J. M. *J. Chem. Soc.* **1963**, *4157*.
(20) Bystrov, V. F. *Prog. Nucl. Magn. Reson. Spectrosc.* **1976**, *10*, 41.

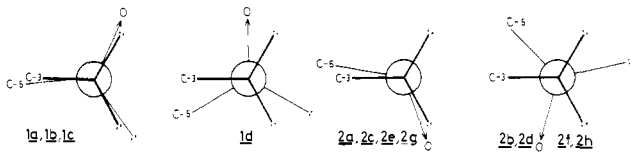

Figure 7. Newman projection along the O2–S1 bond of the conformers of **1** and **2**.

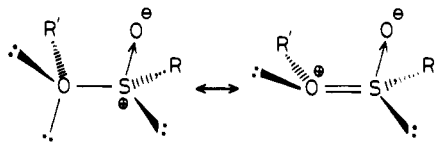

Figure 8. Visualization of the anomeric effect.

given in the preceding section, however, the change in temperature has virtually no effect on the conformation of the sultine ring, inferring that the formation of the intramolecular hydrogen bond does not play a dominant role in determining the conformation of the five-membered ring.

Thus, although the intramolecular hydrogen bond stabilizes the $^4T_5$ conformation of the sultine ring of **1** to a certain extent, we seek the main driving force for this conformation in the so-called gauche effect. This is the well-documented[22,23] preference for gauche over anti geometry in X–C–C–Y fragments in which X and Y represent electronegative substituents. It has been pointed out that the conformational behavior of five-membered ring sugars in nucleosides and nucleotides[5c] as well as in the five-membered proline ring[5d] can be rationalized by assuming a predominant gauche stabilization between the *endocyclic* heteroatom and *exocyclic* substituents. We propose that the conformational behavior of the sultine ring of **1** can be understood in the same way, as in the $^4T_5$ conformation of the sultine ring the exocyclic C–N bond occupies a gauche orientation with respect to the endocyclic C–S and C–O bonds. From the observation that in chloroform no other conformation than the $^4T_5$ conformer could be detected, it follows that the (double) gauche stabilization in the sultine ring amounts to >2 kcal/mol. This lower limit estimate is in accordance with data available[5d] for the gauche effect in N–C–C–O fragments (2.0 kcal/mol), to which the gauche stabilization for the N–C–C–S(O) fragment should be added.

This conformational behavior of **1** changes drastically when the compound was dissolved in Me_2SO-d_6: next to the aforementioned $^4T_5$ conformer **1c** a second conformer **1d** (^3_2T) shows up to an approximately equal extent. This finding may be explained in terms of a diminished gauche effect[24] in the more polar solvent Me_2SO.

In addition, the anomeric effect has to be taken into account. In Figure 7 the Newman projections along the O2–S1 bond of the conformers **1a–d** are depicted. It is noted that in the ^3_2T conformation (**1d**) the S→O bond of the sultine ring approaches an antiperiplanar orientation with respect to one of the ring oxygen lone pairs, suggesting a stabilization on the basis of an anomeric effect.[25,26] In Figure 8 this anomeric effect is visualized. Finally, Me_2SO is a strong hydrogen bond accepting solvent capable of competing with the intramolecular hydrogen bond accepting sulfinyl function. Indeed, a reduced intramolecular hydrogen-bonding tendency is reflected by the relatively low $^3J(H_4–NH)$ value (Table III).

Table VIII. Crystal Data

mol formula	$C_8H_{15}NO_4S$
fw	221.275
cryst system	monoclinic
space group	$P2_1$
a, Å	9.604 (1)
b, Å	11.652 (1)
c, Å	9.949 (1)
β, deg	90.93 (1)
V_{calcd}, Å^3	1113.3
Z	4
D_{calcd}, g cm^{-3}	1.32
$F(000)$	471.9
μ(Cu Kα), cm^{-1}	24.74

In the discussion of the conformational analysis of **2** an additional observation has to be taken into account, viz., the occurrence of a minor ("cis") and a major ("trans") component at low temperature (233 K). Molecules like **1–3** containing a urethane moiety can indeed exist as a pair of rotamers of the C–N–C(O) bond. This has been observed earlier with urethanes in general[27–32] and more particularly with urethanes derived from amino acids,[31–36] amino acid esters,[33,38,39] and peptides[33–39] containing the BOC or CbO group as the N-protecting group. Often the rotamers were found to be present in unequal amounts[29,31,34,36,39] as is the case in this study too. The more stable trans rotamer (Z configuration) will be present in excess over the cis rotamer (E configuration).

The equilibrium between the major and minor component of **2** is slow on the NMR time scale at 233 K, so that the separate rotamers can be observed (Figure 4). At 300 K a situation near coalescence is observed, and at 383 K in $C_2D_2Cl_4$ the interconversion of rotamers is rapid. With the assumption that 300 K is about the temperature of coalescence, a rough estimate for the activation energy of rotation around the C–N bond ($\Delta G^{\ddagger}$) gives a value of 15 kcal/mol. This compares favourably with studies on other urethanes.[27,28,36]

The major as well as the minor component consist of an equilibrium between a twist-chair, **2a,b** (^4_3T), and envelope, **2b,d** ($_1E$), conformer (Scheme II). The twist-chair conformer is present in excess in the minor as well as in the major component (mole fraction 0.76 and 0.91, respectively, see Table VII). We attribute the stabilization of the ^4_3T conformer to a double gauche effect: the C–N bond has a gauche position to the endocyclic C–O and C–S bonds. In the E conformer the only discernible stabilization is the anomeric effect (Figure 7).

Finally, a comparison of the conformations of **2**, which are present in solution (Scheme II), with the solid-state conformation (Figure 3) shows that the latter differs from the conformers in solution. The solid-state conformation is almost envelope-shaped with the C3 atom as the most puckered atom. In contradistinction the conformations in solution are twisted chair (**2a,e,g,c**) or envelope-shaped (**2b,f,h,d**) with the S atom as the puckered atom. Obviously, the intermolecular interactions in the solid state—

(21) At present, no quantitative estimate for the population of the non-hydrogen-bonded species at 300 K can be given, as the conformation(s) of the C4–N bond in the non-hydrogen-bonded state is not known. However, taking the low (theoretical) limiting value of the coupling constant in the latter state to 0.37 Hz (for a H–N–C–H torsion angle of 90° according to Bystrov[20]), the population of the non-hydrogen-bonded state amounts to *at least 20%*.

(22) (a) Eliel, E. L.; Kaloustan, M. K. *J. Chem. Soc., Chem. Commun.* **1970**, 290. (b) Abraham, R. J.; Banks, H. D.; Eliel, E. L.; Hofer, O.; Kaloustan, M. *J. Am. Chem. Soc.* **1972**, *94*, 1913. (c) Eliel, E. L.; Evans, S. A., Jr. *Ibid.* **1972**, *94*, 8588. (d) Eliel, E. L.; Alcadie, F. *Ibid.* **1974**, *96*, 1939.

(23) Abraham, R. J.; Gatti, G. *J. Chem. Soc. B* **1969**, 961.

(24) Examples of a diminished gauche effect in polar vs. apolar solvents—albeit not always interpreted as such—are found in, e.g., several 5-substituted 1,3-dioxanes[22] and 1,2-disubstituted ethanes.[23]

(25) Lemieux, R. U. *Pure Appl. Chem.* **1971**, *25*, 527.

(26) Eliel, E. L. *Angew. Chem.* **1972**, *84*, 779.

(27) Price, B. J.; Smallman, R. V.; Sutherland, I. O. *J. Chem. Soc., Chem. Commun.* **1966**, 319.

(28) Lustig, E.; Benson, W. R.; Duy, N. *J. Org. Chem.* **1967**, *32*, 851.

(29) van der Werf, S.; Engberts, J. D. F. N. *Tetrahedron Lett.* **1968**, 3311.

(30) Kessler, H. *Angew. Chem.* **1970**, *82*, 237.

(31) Stewart, W. E.; Siddall, T. H. *Chem. Rev.* **1970**, *70*, 517.

(32) Yoder, C. H.; Komoriya, A.; Kochanowski, J. E.; Suydam, F. H. *J. Am. Chem. Soc.* **1971**, *93*, 6515.

(33) Dimicoli, J. L.; Ptak, M. *Tetrahedron Lett.* **1970**, 2013.

(34) Branik, H.; Kessler, H. *Tetrahedron* **1974**, *30*, 781.

(35) Branik, H.; Kessler, H. *Chem. Ber.* **1975**, *108*, 2176.

(36) Bats, J. W.; Fuess, H.; Kessler, H.; Schuck, R. *Chem. Ber.* **1980**, *113*, 520.

(37) Kessler, H.; Zimmerman, G.; Förster, H.; Engel, J.; Oepen, G.; Steldrick, W. S. *Angew. Chem.* **1981**, *93*, 1085.

(38) Garner, R.; Watkins, W. B. *J. Chem. Soc., Chem. Commun.* **1969**, 386.

(39) Deber, C. M.; Bovey, F. A.; Carver, J. P.; Blout, E. R. *J. Am. Chem. Soc.* **1970**, *92*, 6191.

Table IX. Final Positional Parameters (×10⁴ for Non-Hydrogen Atoms; ×10³ for H Atoms) and Thermal Parameters (×10²)

molecule 1[a]					molecule 2[b]				
atom	*x*	*y*	*z*	U_{eq}, Å²	atom	*x*	*y*	*z*	U_{eq}, Å²
S1	1192	7241	9819	8.9 (1)	S1′	888	10558	4705	8.4 (1)
C5	2178	7168	8323	7.2 (2)	C5′	1003	9487	3362	8.9 (3)
C4	2075	8334	7631	7.1 (2)	C4′	2477	11102	2873	6.9 (3)
C3	784	8876	8239	10.1 (4)	C3′	2244	9864	2500	6.2 (2)
C8	4131	9236	6760	4.8 (1)	C8′	4338	8888	1776	5.0 (2)
C10	6376	10176	6315	4.9 (2)	C10′	6617	7988	1445	5.0 (2)
C12	7343	10811	7256	7.0 (3)	C12′	7551	7366	2404	7.1 (3)
C13	7045	9124	5768	8.7 (3)	C13′	6089	7170	343	10.0 (3)
C14	5852	10968	5212	7.8 (3)	C14′	7276	9051	920	9.5 (3)
O6	−70	6560	9571	10.6 (3)	O6′	−334	11221	4316	12.3 (3)
O2	844	8562	9624	9.1 (2)	O2′	2279	11197	4262	7.5 (2)
O11	3888	8955	5631	5.9 (2)	O11′	4157	9155	620	7.7 (2)
O9	5224	9837	7209	5.4 (2)	O9′	5412	8313	2275	6.1 (2)
N7	3265	9019	7792	6.6 (2)	N7′	3450	9170	2767	5.8 (2)
H51	325	694	852		H51′	127	865	386	
H52	174	650	764		H52′	6	941	284	
H4	198	826	654		H32′	175	1167	230	
H32	−16	852	773		H31′	353	1138	259	
H31	76	980	807		H4′	195	980	143	
H7	348	935	872		H7′	366	890	370	
H121	824	1114	676		H121′	853	715	194	
H122	681	1155	775		H122′	780	792	328	
H123	772	1027	811		H123′	706	660	277	
H131	630	862	519		H131′	694	678	−17	
H132	793	932	518		H132′	550	646	84	
H133	742	853	659		H133′	539	759	−35	
H141	528	1171	562		H141′	752	962	180	
H142	671	1130	464		H142′	825	885	46	
H143	514	1054	451		H143′	662	952	25	

[a] The numbering of the non-hydrogen atoms is as indicated in Figure 2. The numbering of the hydrogen atoms (not shown in the figure) is determined by the atoms to which they are attached, e.g., H_{121}, H_{122}, and H_{123} denote three protons attached to atom 12, a C atom. [b] H atoms were assigned a fixed *U* value of 9.0 Å². Esd's are between 2×10^{-4} and 9×10^{-4} for non-hydrogen atoms.

especially the intermolecular hydrogen bonding (Figure 1)—force the molecule into a conformation, which does not need to be the most stable one in solution.

In Summary. Both diastereomers **1** and **2** behave in a remarkably consistent way: in $CDCl_3$ the presence of the exocyclic C–N bond dominates the conformational behavior by exerting a (double) gauche stabilization which leads to a $^4T_3$ conformation for **1** and to a (predominant) ^4_3T conformation for **2**. In Me_2SO-d_6 this gauche effect is counterbalanced by the anomeric effect and/or diminished in this more polar solvent.

This study adds a new example[40] to the growing number of compounds showing different conformations in the solid state and in solution. Work is in progress to evaluate the influence of the conformation of functionalized sultines on ring-opening reactions and reactions of the α-sulfinyl carbanion with electrophiles.

Experimental Section

Synthesis. Compounds **1**, **2**, and **3** were synthesized as described before.[2]

(2*R*,4*R*)-4-[(3-Phenylpropanoyl)amino]-1,2-oxathialane 2-Oxide (4). This compound has been prepared from *N*-(3-phenylpropanoyl)-L-cystine methyl ester as described[1] for the preparation of **1** and **2** from the corresponding N-protected cystine ester: R_f 0.19 ($MeOH/CH_2Cl_2$, 5/95, v/v). 500-MHz ^1H NMR ($CDCl_3$, 300 K) δ 2.455 (m, 2 H, $CH_2C(O)$), 2.938 (t, 2 H, $C_6H_5CH_2$), 7.158–7.305 (m, 5 H, C_6H_5), 4.309 (H_{32}), 4.763 (H_{31}), 4.913 (H_4), 3.084 (H_{51}), 3.258 (H_{52}), 5.977 (H_N); coupling constants (Hz), H_{31-4}, 4.60, H_{32-4}; 2.69, H_{51-4}, 6.74, H_{52-4}, 2.89, H_4–N_H, 7.20, H_{31-32}, −9.98, H_{51-52}, −14.06.

^1H NMR Spectroscopy. ^1H NMR spectra at 500 MHz were recorded in the Fourier transform mode on a Bruker WM500 spectrometer interfaced with an ASPECT-2000 computer for data accumulation (32K data points). The spectrometer was field frequency locked on the deuterium resonance of the solvent ($CDCl_3$, $C_2D_2Cl_4$, or Me_2SO-d_6), and the sample temperature was regulated with a VT-1000 temperature controller. If necessary, a Lorentz Gauss transformation was carried out before a Fourier transformation, yielding Gaussian enhanced spectra.[41,42] All relevant spectra were analyzed by standard iterative simulation techniques using the LAOCOON-III-like PANIC program[43] for the above mentioned ASPECT computer.

Chemical shift data (relative to tetramethylsilane as internal reference) and coupling constants for the investigated compounds are presented in Tables II–V. On the basis of the excellent agreement between observed and simulated spectra, the accuracy of the values of the chemical shifts and of the coupling constants can be considered better than 0.001 ppm and 0.1 Hz, respectively.

X-ray Crystallography. A crystal of about 0.05 × 0.05 × 0.40 mm was used for X-ray measurements. The colorless crystals are monoclinic. Unit cell and space group data were obtained from diffractometer measurements. Accurate unit cell dimensions were determined by a least-squares method from 25 general reflections, measured with Cu Kα radiation (graphite crystal monochromator, λ = 1.5418 Å). Crystal data are listed in Table VIII. The intensities of 8098 reflections, the full sphere with $(\sin\theta)/\lambda < 0.600$ Å^{-1}, were measured on a CAD4 diffractometer, using the ω–2θ scan with a scan range of $(0.80 + 0.14 \tan\theta)°$.

Intensity and orientation control reflections were measured every 30 min and used to correct the data for primary beam intensity fluctuations and crystal decay (20%). Point group (2) equivalent reflections were averaged resulting in 4068 independent reflections, 2341 of which were considered "observed", $I > 3\sigma(I)$ counting statistics. Lorentz and polarization corrections were applied but no absorption correction. The structure was solved by direct methods (MULTAN) by using the PDP-8/CSP[44] programs and refined by full-matrix least-squares to an *R* value of 0.08. Then, on the basis of the anomalous dispersion of S, the absolute configuration was established by comparison of the observed and calculated Bijvoet differences.[45] Refinement was continued; hydrogen atoms could be located in a difference Fourier synthesis but were included at calculated positions. Anisotropic thermal parameters were used for all

(40) Recently, striking examples have been published,[37] which show strong similarities with the compounds in this study: *tert*-butyloxycarbonylphenylalanine exists in the crystal as the cis (*E* configuration) rotamer of the urethane bond and in solution almost the only rotamer is the trans (*Z* configuration) rotamer.

(41) Ernst, R. R. *Adv. Magn. Reson.* **1966**, *2*, 1.
(42) Ferrige, A. G.; Lindon, J. C. *J. Magn. Reson.* **1978**, *31*, 337.
(43) PANIC Program: Copyright, Bruker Spectrospin AG, Switzerland.
(44) Gabe, E. J.; Larson, A. C.; Lee, F. L.; Wang, Y., In "The NRC PDP-8 Crystal Structure Package", Chemistry Division, NRC National Research Council: Ottawa, Canada 1978.
(45) Beurskens, G.; Noordik, J. H.; Beurskens, P. T. *Cryst. Struct. Commun.* **1980**, *9*, 23.

non-hydrogen atoms. The quantity minimized was $R = \sum w([F_o] - K[F_c])^2$ with $w = (\sigma_c^2 + 0.0025\sigma(F_o^2))^{-1}$, σ_c^2 from counting statistics. The y coordinate of S1 and the positions of the hydrogen atoms were not allowed to vary. The final R value is 0.051 for 252 variables and 2341 contributing reflections. A final difference map showed no significant resulting density. The atomic scattering factors for S, O, N, and C were those of Cromer and Mann[46] and those of Stewart et al.;[47] the CSP[44] and XRAY[48] programs were used for the calculations. The molecular structure and the atomic numbering are shown in Figure 2. The final atomic parameters are given in Table IX.

Acknowledgment. We thank Prof. C. Altona and Dr. F. A. A. M. de Leeuw for sharing unpublished data and for stimulating discussions. We thank Mr. B. Zweers for preparing compound **4** and Prof. R. J. F. Nivard for reading and critisizing the manuscript. This research was supported by the Netherlands Foundation for Chemical Research (SON) with financial aid from the Netherlands Organization for the Advancement of Pure Research (ZWO). NMR spectra were recorded at the Dutch National 500/200 MHz hf-NMR facility at Nijmegen.

Registry No. 1, 79464-59-8; **2**, 79409-96-4; **3**, 79409-90-8; **4**, 86239-13-6; *N*-(3-phenylpropanoyl)-L-cystine methyl ester, 86259-41-8.

(46) Cromer, D.; Mann, J. *Acta Crystallogr., Sect A* **1968**, *A24*, 321.
(47) Stewart, R. F.; Davidson, E. R.; Simpson, W. T. *J. Chem. Phys.* **1968**, *42*, 3175.
(48) Stewart, J. M.; Machin, P. A.; Dickinson, C.; Ammon, H. L.; Heck, H.; Flack, H. "The X-Ray system—version of 1976"; Techical Report TR-446, Computer Science Center: University of Maryland, College Park, MD, 1976.

Volumetric Study on the 1,3-Dipolar Cycloaddition Reaction. 2.[1] α-Benzoyl-*N*-phenylnitrone with Several Olefins

Y. Yoshimura, J. Osugi, and M. Nakahara*

Contribution from the Department of Chemistry, Faculty of Science, Kyoto University, Kyoto 606, Japan. *Received March 2, 1983*

Abstract: A high-pressure kinetic study was made of the 1,3-dipolar cycloaddition reaction of α-benzoyl-*N*-phenylnitrone (BPN) with dimethyl fumarate (DMF), dimethyl maleate (DMM), methyl acrylate (MA), and styrene (St) in toluene at 25 °C. The activation volumes (ΔV^*) at 1 bar for DMF, DMM, MA, and St are −21.7, −19.9, −22.9, and −19.5 cm^3 mol^{-1}, respectively. The volume change (ΔV) for the reaction between BPN and DMF was determined dilatometrically: $\Delta V = -22.7$ cm^3 mol^{-1} and $\Delta V^*/\Delta V = 0.956$. In order to elucidate the manner in which the activation volume reflects geometrical changes of molecules reacting in the liquid phase, the experimental results are compared with theoretically calculated changes in the van der Waals volume (V_W) for the prototype 1,3-dipolar cycloaddition between HCNO and HCCH: $\Delta V_w^* = -4.0$ cm^3 mol^{-1}, $\Delta V_W = -8.2$ cm^3 mol^{-1}, and $\Delta V_W^*/\Delta V_W = 0.49$. The large gap between ΔV^* and ΔV_W^* and between ΔV and ΔV_W is explained by taking account of the size dependence of the packing coefficient for each species involved in the prototype reaction.

The primary goal of the high-pressure kinetic study on chemical reactions in solution is to account for the reaction mechanism in terms of the activation volume (ΔV^*) obtained from the transition-state theory:[2,3]

$$\Delta V^* = -RT\left(\frac{\partial \ln k}{\partial P}\right)_T + RT\left(\frac{\partial \ln \kappa}{\partial P}\right)_T \quad (1)$$

where R, T, P, k, and κ are the gas constant, the temperature, the pressure, the rate constant (expressed in molality or mole fraction), and the transmission coefficient, respectively; the second term in eq 1 has been assumed to be negligible except for one case.[4] A large number of inorganic[5,6] and organic[7] reactions have been mechanistically studied by using this quantity together with the following additivity postulate:

$$\Delta V^* = \Delta_1 V^* + \Delta_2 V^* \quad (2)$$

where $\Delta_1 V^*$ is the change in volume of the reacting molecules during the activation process and $\Delta_2 V^*$ due to solvation (electrostriction) of ionic or polar species.[2,8] However, it is not yet established how to split ΔV^* into the two components; determination of $\Delta_2 V^*$ depends on how $\Delta_1 V^*$ is estimated and vice versa. In this regard, a thorough study of $\Delta_1 V^*$ is worthwhile.

When we try to examine how $\Delta_1 V^*$ is correlated with structural changes of reacting molecules during the activation step, it is advantageous to select a type of reactions that has negligibly small solvent effect and therefore little contribution of $\Delta_2 V^*$ to ΔV^* in eq 2; here these nonionic reactions are called "molecular" reactions. Although the 1,3-dipolar cycloaddition is one of such molecular reactions, there has been no extensive study of the pressure effect on it. Hence, the present authors attempt to clarify volumetric aspects of the 1,3-dipolar cycloaddition in a series of studies. The first paper[1] in this series has shown that ΔV^* for the 1,3-dipolar cycloaddition of Ph_2CN_2 with six olefins in toluene at 25 °C and 1 bar is in the range of −20 to −24 cm^3 mol^{-1}. In the present work, the 1,3-dipole is changed to α-benzoyl-*N*-phenylnitrone in order to see how far ΔV^* for the 1,3-dipolar cycloaddition is affected by the nature of the 1,3-dipole. It is found here that ΔV^* for

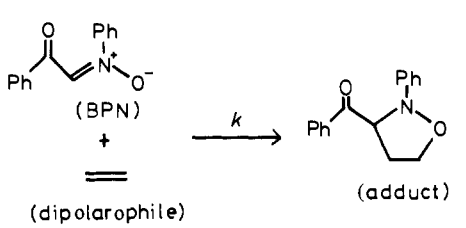

the 1,3-dipolar cycloaddition is little varied from one dipole to another.

How to interpret ΔV^* ($\Delta_1 V^*$) for the molecular reaction in the liquid phase at the molecular level is an open problem. A recent

(1) The previous paper is designated as part 1 of the present series: Yoshimura, Y.; Osugi, J.; Nakahara, M. *Bull. Chem. Soc. Jpn.*, **1983**, *56*, 680.
(2) Evans, M. G.; Polanyi, M. *Trans. Faraday Soc.* **1935**, *31*, 875.
(3) Glasstone, S.; Laidler, K. J.; Eyring, H. "The Theory of Rate Processes"; McGraw-Hill: New York, 1941.
(4) Hasha, D. L.; Eguchi, T.; Jonas, J. *J. Am. Chem. Soc.* **1982**, *104*, 2290.
(5) Eldick, R. v.; Kelm, H. *Rev. Phys. Chem. Jpn.* **1980**, *50*, 185.
(6) Swaddle, T. W. *Rev. Phys. Chem. Jpn.* **1980**, *50*, 230.
(7) Asano, T.; le Noble, W. J. *Chem. Rev.* **1978**, *78*, 407.
(8) (a) Hamman, S. D. "Physico-chemical Effects of Pressure"; Butterworth: London, 1957; Chapter 9. (b) "High Pressure Physics and Chemistry"; Bradley, R. S., Ed.; Academic Press: London, 1963; Vol. 2, Chapter 8.

0002-7863/83/1505-5414$01.50/0